JOURNAL OF VIROLOGY, Feb. 2011, p. 1267–1274 Vol. 85, No. 3
0022-538X/11/$12.00 doi:10.1128/JVI.01717-10

Inhibition of Enveloped Virus Infection of Cultured Cells by Valproic Acid▽†

Ángela Vázquez-Calvo,[1] Juan-Carlos Saiz,[2] Francisco Sobrino,[1,3]* and Miguel A. Martín-Acebes[2]

Centro de Biología Molecular Severo Ochoa (UAM-CSIC), Cantoblanco, Madrid, Spain[1]; Departamento de Biotecnología, Instituto Nacional de Investigación y Tecnología Agraria y Alimentaria, Madrid, Spain[2]; and Centro de Investigación en Sanidad Animal, Instituto Nacional de Investigación y Tecnología Agraria y Alimentaria, Valdeolmos, Madrid, Spain[3]

Received 13 August 2010/Accepted 12 November 2010

Valproic acid (VPA) is a short-chain fatty acid commonly used for treatment of neurological disorders. As VPA can interfere with cellular lipid metabolism, its effect on the infection of cultured cells by viruses of seven viral families relevant to human and animal health, including eight enveloped and four nonenveloped viruses, was analyzed. VPA drastically inhibited multiplication of all the enveloped viruses tested, including the zoonotic lymphocytic choriomeningitis virus and West Nile virus (WNV), while it did not affect infection by the nonenveloped viruses assayed. VPA reduced vesicular stomatitis virus infection yield without causing a major blockage of either viral RNA or protein synthesis. In contrast, VPA drastically abolished WNV RNA and protein synthesis, indicating that this drug can interfere the viral cycle at different steps of enveloped virus infection. Thus, VPA can contribute to an understanding of the crucial steps of viral maturation and to the development of future strategies against infections associated with enveloped viruses.

Conventional antiviral agents can interfere successfully with viral components but often lead to development of drug resistance in virus populations evolving under selective pressures (9, 14). One of the approaches to circumvent this limitation is the identification of antivirals targeted against cellular functions required for the virus to complete its viral cycle, thus reducing the potential of viruses to escape from drug effects (26, 35, 44). Indeed, some long-used drugs commonly administered by clinicians to treat human disorders, such as lithium or statins, have been proposed as new antiviral agent candidates (3, 18, 20) as part of drug repositioning (finding of new applications to licensed drugs) in drug development. Massive screenings have also revealed the potential antiviral effect of multiple clinical compounds, supporting this kind of approach (17).

Valproic acid ([VPA] 2-propylpentanoic acid) is a branched short-chain fatty acid commonly used for treatment of neurological disorders (6, 52). The proposed cellular targets of VPA are diverse, including (i) interruption of γ-amino butyric acid (GABA) signaling, (ii) inhibition of histone deacetylases (HDAC), (iii) modulation of sodium channel activity, (iv) inhibition of glycogen synthase kinase 3, and (v) disruption of membrane lipid metabolism, including that of phosphatidylinositol (48, 53, 54, 57, 59).

As intracellular parasites, many viruses hijack cellular membranes from host cells for virus replication and/or virion assembly, and alterations in the membrane lipid environment can interfere with these processes (22, 43). This prompted us to examine the effect of VPA on the infectivity of different viruses relevant to human and animal health, such as the flaviviruses West Nile virus (WNV) and Usutu virus (USUV), the arenavirus lymphocytic choriomeningitis virus (LCMV), the rhabdovirus vesicular stomatitis virus (VSV), the togaviruses Semliki forest virus (SFV) and Sindbis virus (SINV), the asfivirus African swine fever virus (ASFV), the poxvirus vaccinia virus (VACV), and the picornaviruses foot-and-mouth disease virus (FMDV), encephalomyocarditis virus (EMCV), bovine enterovirus (BEV), and equine rhinitis A virus (ERAV). We observed that VPA caused a drastic reduction of the yield of all enveloped viruses (WNV, USUV, VSV, SFV, SINV, LCMV, VACV, and ASFV) but did not affect the nonenveloped viruses FMDV, EMCV, BEV, and ERAV. We further analyzed the effect of VPA on enveloped virus infections. For this purpose, two viruses, VSV and WNV, whose infectious cycle are well characterized (1, 5, 13, 19, 28, 30, 33, 36, 46) were used. Our results indicate that VPA reduced the yield of these two viruses by more than 7 orders of magnitude; however, while both WNV RNA and protein synthesis were drastically abolished, no major blockage of VSV RNA and protein synthesis was observed, indicating that VPA can interfere at different steps of enveloped virus infection. These results make VPA an interesting drug for understanding the crucial steps of viral maturation and for developing future strategies against infectious diseases associated with enveloped viruses.

MATERIALS AND METHODS

Cells, viruses, antibodies, and reagents. BHK-21 cells (ATCC) and Vero cells (ATCC) were maintained in Dulbecco's modified Eagle's medium (DMEM) (Gibco-BRL, Invitrogen, Carlsbad, CA) supplemented with 5% fetal calf serum (FCS) (Sigma, St. Louis, MO), L-glutamine (2 mM), penicillin (100 U/ml), and streptomycin (100 μg/ml). Type C FMDV C-S8c1 (50), BEV (23), EMCV (47), SFV and SINV (55), VSV Indiana (40), LCMV (37), and Western Reserve VACV (4) viral stocks were grown in BHK-21 cells. USUV (7), WNV (10), ERAV (32), and ASFV strain BA71V (15) stocks were amplified in Vero cells. Antibodies against WNV E glycoprotein from Chemicon (Temecula, CA), acetylated histone H3 (AcH3) from Upstate (Lake Placid, NY), and tubulin (2) were used. The remaining antibodies and stains used have been previously described (38). Valproic acid sodium salt, VPA (Sigma), was directly dissolved in DMEM.

* Corresponding author. Mailing address: Centro de Biología Molecular Severo Ochoa, Nicolás Cabrera 1, UAM, 28049 Madrid, Spain. Phone: 34 91 196 4493. Fax: 34 91 196 4420. E-mail: fsobrino@cbm.uam.es.

† Dedicated to the memory of Rosario Armas-Portela.

▽ Published ahead of print on 24 November 2010.

The effect of VPA in cultured cells was analyzed by trypan blue exclusion (51). Trichostatin A (TSA) (Cell Signaling Technology, Danvers, MA) was prepared in ethanol as a 4 mM stock solution.

Infections and virus titrations. Confluent monolayers (grown in six-well plates) of BHK-21 or Vero cells were extensively washed with DMEM and left untreated or were pretreated with VPA for 10 min. Cells were infected with the different viruses at the selected multiplicity of infection (MOI), defined as the number of PFU/cell. After the first infection hour (or 1.5 h for LCMV) in the presence or absence of VPA, the viral inoculum was removed, the cell monolayer was washed twice with DMEM, and fresh medium containing 5% FCS and VPA was added; this time point was considered 0 h postinfection (p.i.). Seven hours (for FMDV, EMCV, BEV, VSV, SFV, SINV, and VACV) or 24 h (for ERAV, LCMV, WNV, USUV, and ASFV) later infected plates were frozen. To test the effect of the p.i. addition of VPA, the drug was added and maintained from 2.5 h p.i. To analyze the effect of TSA, BHK-21 cells were left untreated or were pretreated with 400 nM TSA for 16 h, as described by the manufacturer. At this time, cells were infected with FMDV, VSV, SFV, SINV, LCMV, or VACV, as described previously, and TSA was maintained throughout the infection period (total TSA treatment of 24 h). For WNV, USUV, and ASFV, Vero cells were treated at the time of infection with 400 nM TSA, and infections were allow to proceed for 24 h. For virus titration, unless otherwise stated, infected plates were subjected to three freeze-thaw cycles, and the total (intracellular and medium-released) virus yield was determined by plaque assay in BHK-21 or Vero cells as described previously (15, 47, 50). Briefly, after the first hour of infection, viral inoculum was removed, and medium containing 0.5% agar, 1% FCS, and DEAE-dextran (0.045 mg/ml) was added. For LCMV, after 1.5 h of infection, the viral inoculum was removed, and medium containing 0.3% agar, 1% FCS, and DEAE-dextran (0.045 mg/ml) was added. For WNV and USUV, after inoculum removal, infections were allowed to proceed in semisolid medium containing 1% low-melting-point agarose and 2% FCS. Plates were incubated at 37°C for 24 h (FMDV, EMCV, and VSV), 48 h (BEV, ERAV, SFV, and SINV), 72 h (VACV, WNV, and USUV) or 1 week (LCMV and ASFV). At this time point, cells were fixed in 4% formaldehyde for 15 min at room temperature and stained with 3% crystal violet in 2% formaldehyde.

Detection of viral RNA and proteins and concentration of viral particles. VSV particles were sedimented from VSV-infected BHK-21 cell medium as described previously (21). For VSV, total (intracellular and extracellular) RNA and extracellular RNA were extracted using Tri-Reagent (Sigma). Samples were 10-fold serially diluted in water, and VSV cDNA was synthesized and amplified by reverse transcription-PCR (RT-PCR) (41). Glyceraldehyde-3-phosphate-dehydrogenase (G3PDH) RNA amplification was used as an internal control for cellular RNA content (16). PCR products were analyzed by agarose gel electrophoresis (2%) and ethidium bromide staining. For WNV, viral RNA was extracted using a NucleoSpin viral RNA isolation kit (Macherey-Nagel, Düren, Germany) and quantified by quantitative RT-PCR as genomic equivalents to the number of PFU/ml by comparison with RNA extracted from titrated samples (27). For VSV protein detection by dot blot, infection medium samples were loaded onto a nitrocellulose membrane, which was blocked, incubated with a guinea pig hyperimmune serum against VSV Indiana and then with horseradish-peroxidase (HRP)-labeled goat anti-guinea pig IgG, and subsequently developed using an ECL kit (Amersham). These antibodies were also used for Western blot detection (38).

TEM and immunofluorescence. Transmission electron microscopy (TEM) and immunofluorescence were performed as previously described (38). To determine the number of infected cells in immunofluorescence assays, three coverslips per time point were examined, and at least 500 cells were counted. The number of viral particles attached to the cell surface/nm was scored using the NeuronJ plug-in (39) of ImageJ software (http://rsbweb.nih.gov/ij/). For negative staining, VSV virions were concentrated from infection medium (21) and fixed with 1% glutaraldehyde. Samples were adsorbed for 3 min to copper grids coated with collodion-carbon and ionized. Grids were negatively stained with 2% uranyl acetate and air dried.

Data analysis. One-way analysis of variance was performed with the statistical package SPSS, version 17.0 (SPSS, Inc., Chicago, IL) for Windows. For multiple comparisons, Bonferroni's correction was applied. Data are presented as means ± standard deviations. Differences were considered statistically significant at a P value of <0.05.

RESULTS

Effect of VPA on viral infection. We first evaluated the viability of BHK-21 and Vero cells treated with the drug (Fig. 1A). The 50% toxic concentration (TC_{50}) was 244 and 280 mM after 8 h of treatment and 178 and 154 mM after 25 h of treatment for BHK-21 and Vero cells, respectively. Microtubules, actin microfilaments, the Golgi complex, and the endoplasmic reticulum architecture were not altered by VPA treatment (Fig. 1B). Next, the effect of treatment with VPA on the viral yield of four nonenveloped and eight enveloped viruses was analyzed (Fig. 2). No statistically significant reduction in the virus yield postinfection was found for any of the nonenveloped viruses. Conversely, complete inhibition, ranging from 6 to 10 orders of magnitude, was observed in the virus yield from infections with the enveloped viruses when VPA was added before infection and maintained throughout the assay, except for VACV, whose yield, albeit reduced by about 4 logs, was not completely inhibited. For the viruses tested on the two cell lines used in this study, the inhibitions observed were similar, regardless of whether VPA was added before infection or postinfection (p.i.), with the only exception being SINV infection of BHK-21 cells, in which p.i. addition of VPA resulted in a reduction of viral titer by 4 orders of magnitude

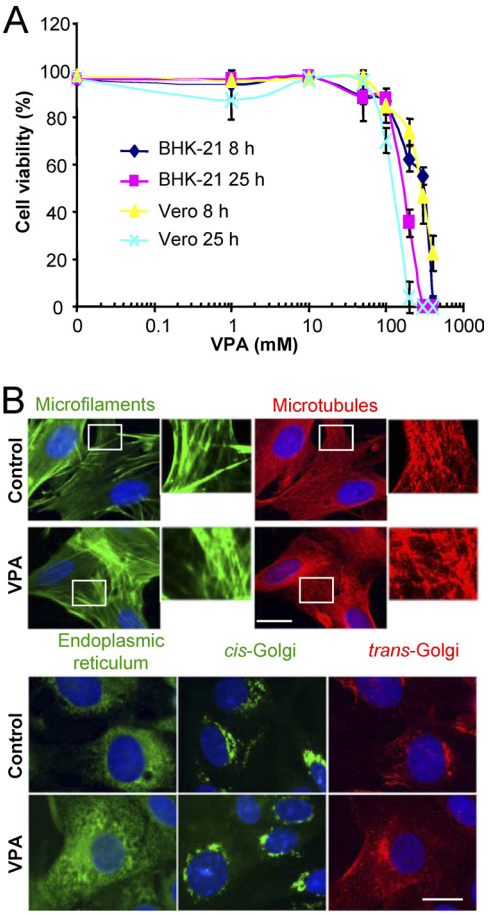

FIG. 1. Effect of VPA on cell viability. (A) BHK-21 and Vero cells were incubated for 8 or 25 h in the presence of increasing concentrations of VPA and then analyzed for cell viability by trypan blue assay. (B) BHK-21 cells, either untreated or treated for 8 h with 50 mM VPA, were fixed and processed for immunofluorescence using antibodies against marker proteins from different cell structures. DAPI (4′,6′-diamidino-2-phenylindole) was used to stain cell nuclei (blue). Scale bar, 20 μm.

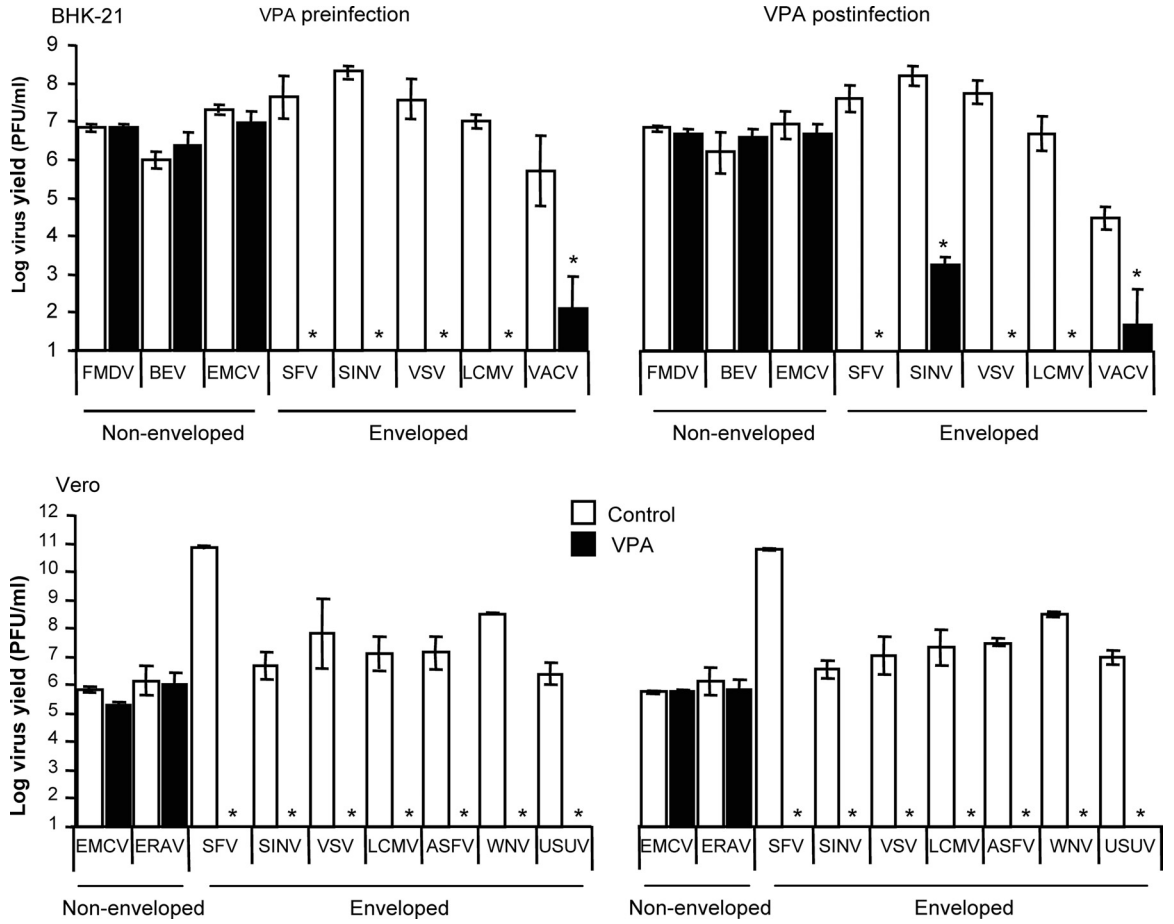

FIG. 2. Effect of VPA on virus yield. BHK-21 or Vero cell monolayers, either untreated or treated with 50 mM VPA, were infected with the indicated viruses (MOI of 0.5 PFU/cell), as described in Materials and Methods. Preinfection analysis corresponds to infections performed in the presence of drug before infection (pretreatment) and throughout the infection time. In the case of postinfection analyses, VPA was added at 2.5 h pi and maintained throughout the infection time. Statistically significant differences between control and VPA-treated cells are indicated by an asterisk ($P \leq 0.05$).

instead of the complete suppression (over 7 orders of magnitude) observed on Vero cells. Overall, these results indicate that VPA affects mainly postentry steps in the multiplication of the enveloped viruses analyzed in the present study.

Inhibition of histone deacetylases does not affect viral infection. Inhibition of histone deacetylases is one of the effects of VPA on cells (54, 57), which has been proposed to have an antiviral effect on latent infections (11, 29, 31, 61). To address the implication of this mechanism on the inhibition observed in this study, the effect of TSA—another HDAC inhibitor (8)—on the infection of FMDV, SFV, SINV, VSV, VACV, LCMV, ASFV, WNV, and USUV was tested. As expected, treatment with TSA resulted in an increase in the levels of the acetylated histone AcH3 (Fig. 3A). However, TSA did not significantly affect infection of the viruses tested (Fig. 3B), supporting the idea that this mechanism does not play a major role on the antiviral effect exerted by VPA.

VPA inhibits viral infection in a dose-dependent manner without drastically inactivating viral particles. From the analysis of the effect of VPA on viral growth, 50% inhibitory concentrations (IC_{50}s) of 0.6 and 0.25 mM were determined for VSV and WNV, respectively (Fig. 4A and C). To asses a possible direct effect of VPA on the infectivity of viral particles, as described for other antiviral drugs directed against enveloped viruses (58), equal numbers of PFU were treated with VPA, and the infectivity levels of the samples were determined by plaque assay after incubation at 37°C for up to 8 h (Fig. 4B and D). While no statistically significant differences were found in the VSV titers observed in control and VPA-treated samples (Fig. 4B), a reduction of 2 orders of magnitude was observed for WNV (Fig. 4D). These results indicate that VPA, although differentially affecting VSV and WNV viral particles, does not produce a major effect on the infectivity of the viral particles, and they suggest that VPA inhibition of viral yield is mainly mediated by intracellular alterations of infected cells.

Effect of VPA on viral replication. A concentration of 50 mM VPA that completely abolished viral production (Fig. 2) was used to perform a time course analysis of VSV and WNV virus production, protein expression, and RNA synthesis (Fig. 5). As expected, while infectious virus was recovered shortly after infection in control cells, no infectious virus was detected in VPA-treated cells infected with either VSV or WNV up to 8.5 and 24 h p.i., respectively (Fig. 5A and D). Upon WNV infection, fluorescence against WNV E protein and viral RNA, the

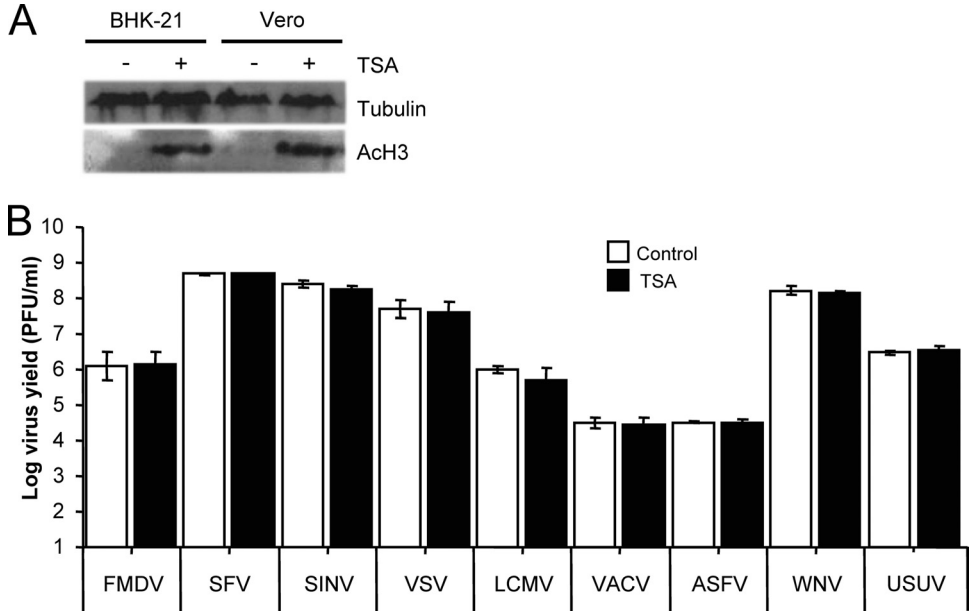

FIG. 3. Inhibition of histone deacetylases does not affect viral infection. (A) Western blot analysis of acetylated histone H3 (AcH3) in BHK-21 and Vero cells after TSA treatment. Results obtained with an anti-β-tubulin antibody are shown as a control for protein loading. (B) BHK-21 or Vero cell monolayers, either untreated or treated with 400 nM TSA, were infected with FMDV, SFV, SINV, VSV, LCMV, VACV, ASFV, WNV, or USUV (MOI of 0.5 PFU/cell). Virus yield was determined by plaque assay as described in Materials and Methods.

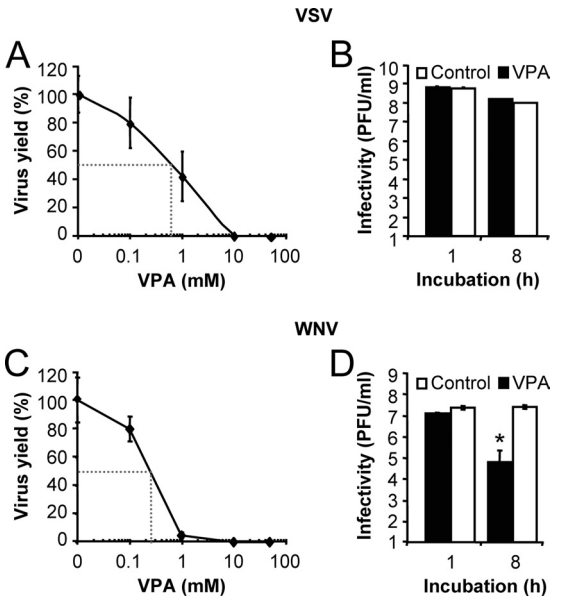

FIG. 4. VPA inhibits VSV and WNV infection in a dose-dependent manner, but VPA treatment does not inactivates VSV particles even though it reduces the infectivity of WNV particles. (A) BHK-21 cells were infected with VSV (MOI of 0.5 PFU/cell) in the presence of different concentrations of VPA, and the total virus yield was determined by plaque assay. Dotted lines correspond to IC_{50}s. (B) VSV particles were incubated with 50 mM VPA at 37°C for 1 h or 8 h, and virus titer was determined by plaque assay. (C) Vero cells were infected with WNV as described in panel A. Dotted lines correspond to IC_{50}s. (D) WNV particles were incubated with VPA as described in panel B, and infectivity was determined by plaque assay. Statistically significant differences between control and VPA-treated cells are indicated by an asterisk ($P \leq 0.05$).

latter being amplified in control cells from 16 h p.i, was not detected in VPA-treated cells at any time point (Fig. 5B and C). In contrast, a reduced percentage of cells positive for fluorescence against the VSV G glycoprotein (VSV-G) was found in VSV-infected cells treated with VPA, and only control cells, not VPA-treated cells, showed a marked increase in the percentage of fluorescent cells from 4.5 h p.i., a time at which untreated cells were actively producing new viruses (Fig. 5D and E). These results suggest that VSV progeny from control cells but not from VPA-treated cells was released to the infection medium and infected neighbor cells. Likewise, in total RNA (intracellular and extracellular) from control VSV-infected cells, viral RNA was already detected at 4.5 h p.i while in VPA-treated VSV-infected cells, viral RNA detection was delayed until 6.5 h. p.i., and the levels were lower than those observed in nontreated control cells (Fig. 5F). On the other hand, no differences were found in the intracellular distribution pattern of VSV-G protein between control cells and those treated with VPA that were positive for VSV-G staining (Fig. 5G). VSV-G protein was observed perinuclearly at 2.5 h p.i., indicating its accumulation in the Golgi complex; at later infection stages (6.5 h p.i.) this protein was observed at the cell periphery, where newly synthesized virions acquire their envelope. When the VSV proteins were detected in infected cells by Western blotting using a polyclonal VSV serum, a reduction of about 10-fold was noticed in the amount of protein N found in VPA-treated cells relative to that of control infected cells (Fig. 5H). Whether the differences observed in VSV RNA and protein detection are due to a reduction in their synthesis in VPA-treated cells and/or to the increasing number of infected control cells remains to be determined. Thus, even though no infective viruses are released from either WNV- or VSV-infected cells, VPA intracellular effects on the infectivity of both

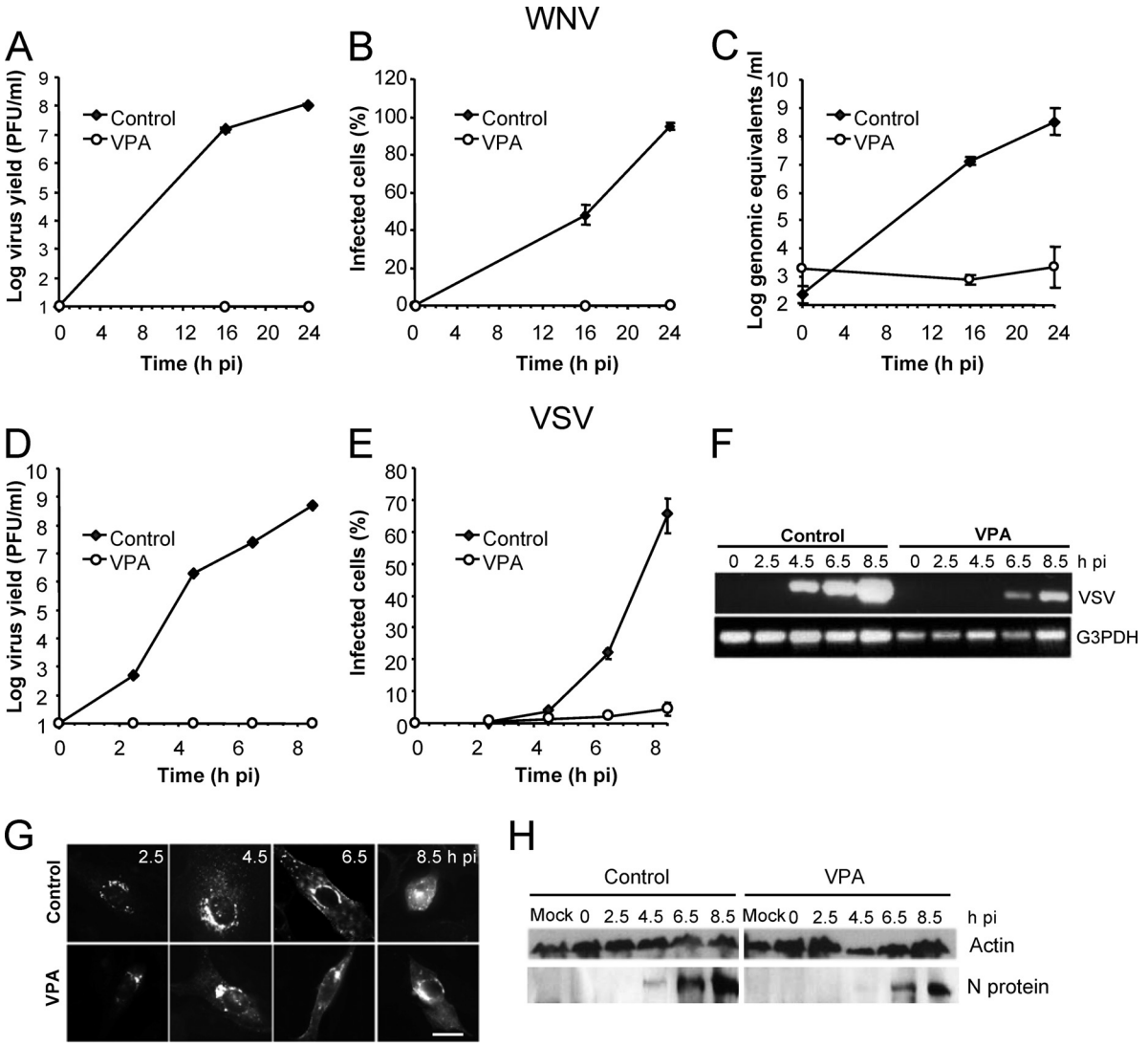

FIG. 5. Effect of VPA on VSV and WNV infection. (A) Vero cells, either untreated or treated with 50 mM VPA, were infected with WNV (MOI of 0.5 PFU/cell), and the virus titer in the extracellular medium was determined by plaque assay. (B) Cells infected as described in panel A were fixed at different times p.i. and processed for immunofluorescence using a MAb against WNV-E glycoprotein. For each time point, the percentage of fluorescent cells (infected cells) is shown. (C) Total viral RNA (intracellular and extracellular) from samples infected with WNV as described in panel A was extracted at different times p.i. and amplified by quantitative RT-PCR as described in Materials and Methods. (D) BHK-21 cells were infected with VSV, and the virus titer in the extracellular medium was determined as in panel A. (E) Cells infected with VSV and processed as described in panel B using MAb I1 against VSV-G protein. (F) Detection of VSV RNA by RT-PCR. BHK-21 cell monolayers were infected with VSV as in panel A. Total viral RNA was amplified by RT-PCR. G3PDH amplification was used as an internal control for cellular RNA content. (G) Representative micrographs of VSV-G-positive cells infected and immunostained as described in panel E. Scale bar, 20 μm. (H) Detection of VSV proteins by Western blotting. BHK-21 cell monolayers were infected with VSV as in panel A. For each time point, cells were lysed and processed for Western blotting using a guinea pig hyperimmune serum against VSV Indiana. The migration of the band shown corresponded to that expected for VSV N protein. Results obtained with an anti-β-actin antibody are shown as a control for protein loading.

viruses seem to differ. Taken together, these results indicate that while in some viruses, such as WNV, VPA can produce a drastic blockage of replication and translation of viral RNA, in other viruses (VSV) this reduction is less severe.

Effect of VPA on VSV morphogenesis. Since in VPA-treated cells infected by VSV, G protein was observed at the cell periphery, where newly synthesized virions acquire their envelope, we further analyzed whether VPA treatment interfered with viral particle formation and egress. To this purpose, BHK-21 cells, treated or not with this drug, were infected with VSV, fixed, and processed for TEM. In both cases, similar images corresponding to newly assembled VSV particles (60) could be observed (Fig. 6A). When the number of viral particles/μm of membrane was quantified, no significant differences between control and VPA-treated cells were found (Table 1). Similarly, no significant differences in the lengths and diameters of the budding VSV particles were found between VPA-treated and untreated infected cells, indicating that VPA does

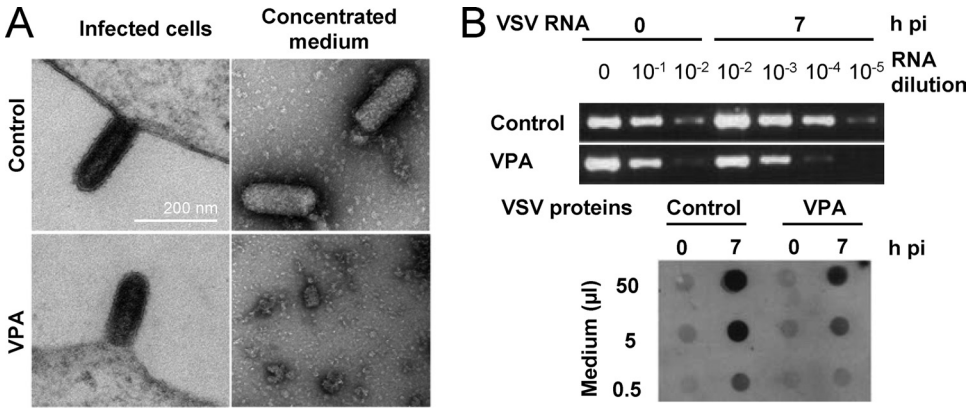

FIG. 6. Effect of VPA on VSV particle morphogenesis. (A) BHK-21 cells, either untreated or treated with 50 mM VPA, were infected with VSV (MOI of 70 PFU/cell). Cells were fixed and processed for TEM at 7 h p.i. (left panels). VSV particles released to infection medium were concentrated and processed for TEM (right panels). Scale bar, 200 nm. (B) VSV RNA amplification by RT-PCR and dot blot detection of VSV proteins in extracellular medium of infected cells described in panel A.

not cause a major blockage of intracellular VSV particle formation. To analyze whether the *de novo* synthesized viral particles were actually released from VPA-treated cells, medium from infected cultures, treated or not with VPA, was sedimented under conditions used for VSV purification. In control infections, bullet-shaped particles corresponding to VSV virions were observed by TEM in resuspended pellets (an average of 31 ± 9.2 particles/field in 20 random fields). None particles of this type were found in the 20 random fields from VPA-treated infected cells (Fig. 6A), suggesting that VPA treatment could either block virion budding or alter VSV composition, producing virions with a highly reduced stability in the infection medium and/or during the sedimentation process. As shown in Fig. 6B, the latter possibility seems to be favored since VSV RNA and proteins were detected in the extracellular medium of infection at levels only about 10-fold lower than those found in control infected cells.

DISCUSSION

In this study we describe the antiviral effect of VPA on different enveloped viruses causing human and veterinary diseases, including important zoonoses such as those caused by WNV and LCMV. Thus, cell culture infection of enveloped viruses whose genomes consist of RNA of positive polarity (WNV, USUV, SFV, and SINV), negative polarity (VSV), and segmented and negative polarity (LCMV), as well as of DNA (ASFV), was completely inhibited by VPA and that of the DNA virus VACV was severely reduced. In general, the inhibitions observed in BHK-21 and Vero cells were similar, suggesting that the alterations produced by VPA that mediate its antiviral activity affect common steps of mammalian cell metabolism. However, the differential inhibition of SINV multiplication in BHK-21 and Vero cells when VPA was added after virus entry indicates that the inhibition by VPA may also be modulated by the cell type infected. In contrast, no significant inhibitory effect was observed for nonenveloped viruses such as FMDV, EMCV, BEV, and ERAV.

As noted in the introduction, different effects have been described for VPA, which complicates the analysis and interpretation of the inhibitions observed. One such effect is the inhibition of histone deacetylases, which has been proposed to favor depletion of cells latently infected with human immunodeficiency virus (29), human T-cell leukemia virus type-1 (31), and Epstein-Barr virus (11, 61). The lack of effect of the drug TSA, which inhibits deacetylation of histones, on the infections of the viruses studied indicates that this mechanism does not play a major role in the observed antiviral effect of VPA. On the other hand, a number of studies have shown that VPA affects the lipid composition of cellular membranes (48, 52, 53, 59). Viruses acquire their lipid envelope from membranes of host cells. For instance, flaviviruses, such as WNV and USUV, acquire their envelope from intracellular membranes such as those from the endoplasmic reticulum (56), while in other viruses, such as VSV and SFV, the lipid composition of the

TABLE 1. Effect of VPA treatment on the frequency and size of VSV budding particles in infected cells

Parameter	Value for the group		*P*
	Control cells	VPA-treated cells	
Frequency of VSV budding[a]	$3.67 \times 10^{-3} \pm 0.0136$	$4.65 \times 10^{-3} \pm 0.0178$	0.826
Avg particle size (nm)[b]			
Length	160.61 ± 35.57	144.61 ± 38.00	0.088
Diam	63.01 ± 10.50	63.29 ± 8.46	0.394

[a] Average number of budding viral particles/μm of cell surface (number of cell surfaces scored, 29).
[b] Average size of budding VSV particles was determined by measuring 57 particles from control cells and 24 particles from VPA-treated cells.

virus particles strongly resembles that of the plasma membrane of the cells used for virus growth (24). Therefore, the inhibitory effect of VPA on enveloped virus multiplication described here could be due to alterations in cellular membrane composition that would result in impairment of infectious particle production. Indeed, targeting plasma membrane anionic phospholipids has been revealed as a promising new antiviral strategy (49). Our results indicate that VPA completely blocks WNV RNA and protein synthesis; whether this effect is associated with alterations of endomembranes that could impair viral RNA translation and/or replication or other cell effects of VPA remains to be determined. Conversely, VPA did not cause a major blockage of VSV RNA and protein synthesis as cells positive for VSV-G protein were detected in immunofluorescence studies (Fig. 5E and G), and only a limited (about 10-fold) reduction was observed in the amount of viral RNA and proteins in infected cells. In these experiments, the increase in the percentage of VSV-positive cells noticed in control monolayers was not observed in cells treated with VPA (Fig. 5E), indicating that in the latter no infectious particles are released from initially infected cells. Since VSV and other enveloped viral particles acquire their envelope from the plasma membrane (34), VPA treatment could impair this process due to alterations in the plasma membrane lipid composition (48, 53, 59). However, comparable frequencies of budding particles similar in size and length to those observed in control cells were found in VPA-treated cells, suggesting that VPA does not severely impair VSV particle assembly. Nevertheless, when we attempted to concentrate VSV virions from infected cells, virion-like particles were not detected in purified supernatants from VPA-treated cells. The detection of VSV RNA and viral proteins in the extracellular medium of infection, at levels only 10-fold lower than those found in control infected cells, suggests that, rather than blocking virion budding, VPA treatment alters VSV composition so as to leave extracellular particles with a highly reduced stability. Overall, our results indicate that at least two different mechanisms are involved in the inhibition exerted by VPA on VSV and WNV cell culture infection, and they point out that further experiments are required to characterize these mechanisms and to extend these studies to other viruses inhibited by this drug.

The present results raise the possibility of the therapeutic antiviral potential of VPA, a widely used drug for nervous disorders, including chronic treatments. Although the use of a known drug that affects the nervous system as an antiviral would require determining possible side effects, it could also favor inhibition of neurotropic viruses such as WNV. Indeed, in animal models VPA concentration in plasma positively correlates with that found in the brain (42, 45). VPA doses usually administered to humans are dependent on the body mass, with a therapeutic range for epilepsy treatment of 50 to 100 mg/liter (about 0.3 to 0.6 mM) in plasma (12, 25). These plasma concentrations are very close to the IC_{50}s determined in our work for VSV and WNV (0.6 and 0.25, respectively), supporting a potential antiviral effect *in vivo*. For hypothetical therapeutic applications, VPA pharmacokinetics should also be considered. This drug is metabolized by linear kinetics and its half-life (in adults receiving monotherapy) ranges between 12 ± 6 and 15 ± 2.5 h, although due to the relatively rapid decrease in serum concentrations of VPA, periodic doses should be administered (25). Experiments in animal models are now being designed to assess whether VPA can interfere viral infection *in vivo*.

In summary, VPA is a potent inhibitor of virus multiplication in cultured cells of the enveloped viruses analyzed here, including viruses of the *Flaviviridae* and *Arenaviridae* families, which comprise a number of important human pathogens responsible for diseases such as yellow fever, dengue fever, hepatitis C, and hemorrhagic fevers. Even if further studies with a wider range of virus families are required to address the antiviral spectrum of VPA, our results indicate that VPA may help shed light on the crucial steps of envelope virus maturation and that it might be a potential candidate for development as an antiviral drug either alone or as coadjuvant in combined therapies.

ACKNOWLEDGMENTS

We thank E. Domingo, J. Ortín, E. Tabarés, M. A. Martínez, F. Gavilanes, A. Rodríguez, M. Sáiz, I. Ventoso, L. Carrasco, C. A Hartley, A. L. Carrascosa, I. V. Sandoval, E. Blanco, and M. T. Rejas for providing us with viruses, reagents, and scientific advice.

This work was supported by grants BIO2008-0447-C03-01, CSD2006-0007, SAF2008-04232, FIS-PI071310, FAU2008-0006, and NADIR-UE-228394 and by an institutional grant from the Fundación Ramón Areces.

REFERENCES

1. **Albertini, A. A., G. Schoehn, W. Weissenhorn, and R. W. Ruigrok.** 2008. Structural aspects of rabies virus replication. Cell Mol. Life Sci. **65:**282–294.
2. **Armas-Portela, R., M. A. Parrales, J. P. Albar, A. C. Martinez, and J. Avila.** 1999. Distribution and characteristics of betaII tubulin-enriched microtubules in interphase cells. Exp. Cell Res. **248:**372–380.
3. **Asenjo, A., J. C. Gonzalez-Armas, and N. Villanueva.** 2008. Phosphorylation of human respiratory syncytial virus P protein at serine 54 regulates viral uncoating. Virology **380:**26–33.
4. **Blasco, R., and B. Moss.** 1992. Role of cell-associated enveloped vaccinia virus in cell-to-cell spread. J. Virol. **66:**4170–4179.
5. **Brinton, M. A.** 2002. The molecular biology of West Nile Virus: a new invader of the western hemisphere. Annu. Rev. Microbiol. **56:**371–402.
6. **Bruni, J., and B. J. Wilder.** 1979. Valproic acid. Review of a new antiepileptic drug. Arch. Neurol. **36:**393–398.
7. **Buckley, A., et al.** 2003. Serological evidence of West Nile virus, Usutu virus and Sindbis virus infection of birds in the UK. J. Gen. Virol. **84:**2807–2817.
8. **Codd, R., N. Braich, J. Liu, C. Z. Soe, and A. A. Pakchung.** 2009. Zn(II)-dependent histone deacetylase inhibitors: suberoylanilide hydroxamic acid and trichostatin A. Int. J. Biochem. Cell Biol. **41:**736–739.
9. **Colman, P. M.** 2009. New antivirals and drug resistance. Annu. Rev. Biochem. **78:**95–118.
10. **Cordoba, L., E. Escribano-Romero, A. Garmendia, and J. C. Saiz.** 2007. Pregnancy increases the risk of mortality in West Nile virus-infected mice. J. Gen. Virol. **88:**476–480.
11. **Countryman, J. K., L. Gradoville, and G. Miller.** 2008. Histone hyperacetylation occurs on promoters of lytic cycle regulatory genes in Epstein-Barr virus-infected cell lines which are refractory to disruption of latency by histone deacetylase inhibitors. J. Virol. **82:**4706–4719.
12. **Cramer, J. A., R. H. Mattson, D. M. Bennett, and C. T. Swick.** 1986. Variable free and total valproic acid concentrations in sole- and multi-drug therapy. Ther. Drug Monit. **8:**411–415.
13. **de Silva, A. M., W. E. Balch, and A. Helenius.** 1990. Quality control in the endoplasmic reticulum: folding and misfolding of vesicular stomatitis virus G protein in cells and in vitro. J. Cell Biol. **111:**857–866.
14. **Domingo, E., and J. Gomez.** 2007. Quasispecies and its impact on viral hepatitis. Virus Res. **127:**131–150.
15. **Enjuanes, L., A. L. Carrascosa, M. A. Moreno, and E. Vinuela.** 1976. Titration of African swine fever (ASF) virus. J. Gen. Virol. **32:**471–477.
16. **Garcia-Briones, M. M., et al.** 2004. Immunogenicity and T cell recognition in swine of foot-and-mouth disease virus polymerase 3D. Virology **322:**264–275.
17. **Gastaminza, P., C. Whitten-Bauer, and F. V. Chisari.** 2010. Unbiased probing of the entire hepatitis C virus life cycle identifies clinical compounds that target multiple aspects of the infection. Proc. Natl. Acad. Sci. U. S. A. **107:**291–296.
18. **Gilbert, C., M. Bergeron, S. Methot, J. F. Giguere, and M. J. Tremblay.** 2005. Statins could be used to control replication of some viruses, including HIV-1. Viral Immunol. **18:**474–489.

19. **Gillespie, L. K., A. Hoenen, G. Morgan, and J. M. Mackenzie.** 2010. The endoplasmic reticulum provides the membrane platform for biogenesis of the flavivirus replication complex. J. Virol. **84:**10438–10447.
20. **Gower, T. L., and B. S. Graham.** 2001. Antiviral activity of lovastatin against respiratory syncytial virus in vivo and in vitro. Antimicrob. Agents Chemother. **45:**1231–1237.
21. **Hackett, A. J., F. L. Schaffer, and S. H. Madin.** 1967. The separation of infectious and autointerfering particles in vesicular stomatitis virus preparations. Virology **31:**114–119.
22. **Hsu, N. Y., et al.** 2010. Viral reorganization of the secretory pathway generates distinct organelles for RNA replication. Cell **141:**799–811.
23. **Jimenez-Clavero, M. A., et al.** 2005. Survey of bovine enterovirus in biological and environmental samples by a highly sensitive real-time reverse transcription-PCR. Appl. Environ. Microbiol. **71:**3536–3543.
24. **Kalvodova, L., et al.** 2009. The lipidomes of vesicular stomatitis virus, Semliki forest virus, and the host plasma membrane analyzed by quantitative shotgun mass spectrometry. J. Virol. **83:**7996–8003.
25. **Kanner, A. M.** 2003. The pharmacology of parenteral valproate. Epilepsy Curr. **3:**109–111.
26. **Khattab, M. A.** 2009. Targeting host factors: a novel rationale for the management of hepatitis C virus. World J. Gastroenterol. **15:**3472–3479.
27. **Lanciotti, R. S., et al.** 2000. Rapid detection of West Nile virus from human clinical specimens, field-collected mosquitoes, and avian samples by a TaqMan reverse transcriptase-PCR assay. J. Clin. Microbiol. **38:**4066–4071.
28. **Le Blanc, I., et al.** 2005. Endosome-to-cytosol transport of viral nucleocapsids. Nat. Cell Biol. **7:**653–664.
29. **Lehrman, G., et al.** 2005. Depletion of latent HIV-1 infection in vivo: a proof-of-concept study. Lancet **366:**549–555.
30. **Letchworth, G. J., L. L. Rodriguez, and J. Del Cbarrera.** 1999. Vesicular stomatitis. Vet. J. **157:**239–260.
31. **Lezin, A., et al.** 2007. Histone deacetylase mediated transcriptional activation reduces proviral loads in HTLV-1 associated myelopathy/tropical spastic paraparesis patients. Blood **110:**3722–3728.
32. **Li, F., G. F. Browning, M. J. Studdert, and B. S. Crabb.** 1996. Equine rhinovirus 1 is more closely related to foot-and-mouth disease virus than to other picornaviruses. Proc. Natl. Acad. Sci. U. S. A. **93:**990–995.
33. **Lichty, B. D., A. T. Power, D. F. Stojdl, and J. C. Bell.** 2004. Vesicular stomatitis virus: re-inventing the bullet. Trends Mol. Med. **10:**210–216.
34. **Luan, P., L. Yang, and M. Glaser.** 1995. Formation of membrane domains created during the budding of vesicular stomatitis virus. A model for selective lipid and protein sorting in biological membranes. Biochemistry **34:** 9874–9883.
35. **Ludwig, S.** 2009. Targeting cell signalling pathways to fight the flu: towards a paradigm change in anti-influenza therapy. J. Antimicrob. Chemother. **64:**1–4.
36. **Mackenzie, J. M., and E. G. Westaway.** 2001. Assembly and maturation of the flavivirus Kunjin virus appear to occur in the rough endoplasmic reticulum and along the secretory pathway, respectively. J. Virol. **75:**10787–10799.
37. **Martin, V., A. Grande-Perez, and E. Domingo.** 2008. No evidence of selection for mutational robustness during lethal mutagenesis of lymphocytic choriomeningitis virus. Virology **378:**185–192.
38. **Martin-Acebes, M. A., et al.** 2008. Subcellular distribution of swine vesicular disease virus proteins and alterations induced in infected cells: a comparative study with foot-and-mouth disease virus and vesicular stomatitis virus. Virology **374:**432–443.
39. **Meijering, E., et al.** 2004. Design and validation of a tool for neurite tracing and analysis in fluorescence microscopy images. Cytometry A **58:**167–176.
40. **Novella, I. S., et al.** 1996. Large-population passages of vesicular stomatitis virus in interferon-treated cells select variants of only limited resistance. J. Virol. **70:**6414–6417.
41. **Nunez, J. I., et al.** 1998. A RT-PCR assay for the differential diagnosis of vesicular viral diseases of swine. J. Virol. Methods **72:**227–235.
42. **Ohdo, S., S. Nakano, and N. Ogawa.** 1988. Chronopharmacological study of sodium valproate in mice: dose-concentration-response relationship. Jpn. J. Pharmacol. **47:**11–19.
43. **Ono, A., S. D. Ablan, S. J. Lockett, K. Nagashima, and E. O. Freed.** 2004. Phosphatidylinositol (4,5) bisphosphate regulates HIV-1 Gag targeting to the plasma membrane. Proc. Natl. Acad. Sci. U. S. A. **101:**14889–14894.
44. **Pereira, A. A., and I. M. Jacobson.** 2009. New and experimental therapies for HCV. Nat. Rev. Gastroenterol. Hepatol. **6:**403–411.
45. **Pollack, G. M., and D. D. Shen.** 1985. A timed intravenous pentylenetetrazol infusion seizure model for quantitating the anticonvulsant effect of valproic acid in the rat. J. Pharmacol. Methods **13:**135–146.
46. **Rodriguez, L. L.** 2002. Emergence and re-emergence of vesicular stomatitis in the United States. Virus Res. **85:**211–219.
47. **Rosas, M. F., et al.** 2008. Susceptibility to viral infection is enhanced by stable expression of 3A or 3AB proteins from foot-and-mouth disease virus. Virology **380:**34–45.
48. **Shaltiel, G., et al.** 2004. Valproate decreases inositol biosynthesis. Biol. Psychiatry **56:**868–874.
49. **Soares, M. M., S. W. King, and P. E. Thorpe.** 2008. Targeting inside-out phosphatidylserine as a therapeutic strategy for viral diseases. Nat. Med. **14:**1357–1362.
50. **Sobrino, F., M. Davila, J. Ortin, and E. Domingo.** 1983. Multiple genetic variants arise in the course of replication of foot-and-mouth disease virus in cell culture. Virology **128:**310–318.
51. **Strober, W.** 2001. Trypan blue exclusion test of cell viability. Curr. Protoc. Immunol. **Appendix 3:**Appendix 3B.
52. **Terbach, N., and R. S. Williams.** 2009. Structure-function studies for the panacea, valproic acid. Biochem. Soc. Trans. **37:**1126–1132.
53. **Tokuoka, S. M., A. Saiardi, and S. J. Nurrish.** 2008. The mood stabilizer valproate inhibits both inositol- and diacylglycerol-signaling pathways in *Caenorhabditis elegans*. Mol. Biol. Cell **19:**2241–2250.
54. **Venkataramani, V., et al.** 2010. Histone deacetylase inhibitor valproic acid inhibits cancer cell proliferation via down-regulation of the Alzheimer amyloid precursor protein. J. Biol. Chem. **285:**10678–10689.
55. **Ventoso, I., et al.** 2006. Translational resistance of late alphavirus mRNA to eIF2α phosphorylation: a strategy to overcome the antiviral effect of protein kinase PKR. Genes Dev. **20:**87–100.
56. **Welsch, S., et al.** 2009. Composition and three-dimensional architecture of the dengue virus replication and assembly sites. Cell Host Microbe **5:**365–375.
57. **Wittenburg, L. A., L. Bisson, B. J. Rose, C. Korch, and D. H. Thamm.** 2010. The histone deacetylase inhibitor valproic acid sensitizes human and canine osteosarcoma to doxorubicin. Cancer Chemother. Pharmacol. doi:10.1007/s00280-010-1287-z.
58. **Wolf, M. C., et al.** 2010. A broad-spectrum antiviral targeting entry of enveloped viruses. Proc. Natl. Acad. Sci. U. S. A. **107:**3157–3162.
59. **Xu, X., et al.** 2007. Attenuation of phospholipid signaling provides a novel mechanism for the action of valproic acid. Eukaryot. Cell **6:**899–906.
60. **Zajac, B. A., and K. Hummeler.** 1970. Morphogenesis of the nucleoprotein of vesicular stomatitis virus. J. Virol. **6:**243–252.
61. **Zhou, J., A. R. Snyder, and P. M. Lieberman.** 2009. Epstein-Barr virus episome stability is coupled to a delay in replication timing. J. Virol. **83:** 2154–2162.